Reproducible and efficient generation of functionally active neurons from human hiPSCs for preclinical disease modeling

Yunyao Xie[a,1], **Ryan J. Schutte**[a,1], **Nathan N. Ng**[a,1], **Kevin C. Ess**[b], **Philip H. Schwartz**[c], and **Diane K. O'Dowd**[a,*]

[a]Department of Developmental and Cell Biology, University of California, Irvine, Irvine, CA, United States

[b]Department of Pediatrics, Vanderbilt University Medical Center, Nashville, TN, United States

[c]Children's Hospital of Orange County Research Institute, Orange, CA, United States

Abstract

The use of human induced pluripotent stem cell (hiPSC)-derived neuronal cultures to study the mechanisms of neurological disorders is often limited by low efficiency and high variability in differentiation of functional neurons. Here we compare the functional properties of neurons in cultures prepared with two hiPSC differentiation protocols, both plated on astroglial feeder layers. Using a protocol with an expandable intermediate stage, only a small percentage of cells with neuronal morphology were excitable by 21–23 days in culture. In contrast, a direct differentiation strategy of the same hiPSC line produced cultures in which the majority of neurons fired action potentials as early as 4–5 days. By 35–38 days over 80% of the neurons fired repetitively and many fired spontaneously. Spontaneous post-synaptic currents were observed in ~40% of the neurons at 4–5 days and in ~80% by 21–23 days. The majority (75%) received both glutamatergic and GABAergic spontaneous postsynaptic currents. The rate and degree of maturation of excitability and synaptic activity was similar between multiple independent platings from a single hiPSC line, and between two different control hiPSC lines. Cultures of rapidly functional neurons will facilitate identification of cellular mechanisms underlying genetically defined neurological disorders and development of novel therapeutics.

Keywords

Induced pluripotent stem cells; hiPSC-derived neurons; Functional differentiation; Reproducibility; Disease modeling

1. Introduction

Neuronal cultures derived from human hiPSCs are a useful model system for exploring cellular mechanisms underlying the pathogenesis of neurological disorders and for

[*]Corresponding author at: 4221 McGaugh Hall, University of California, Irvine, Irvine, CA 92697, United States. dkodowd@uci.edu (D.K. O'Dowd).

[1]Authors contributed equally.

developing novel therapies. Analyses of hiPSC-derived neurons from patients with defined neurological diseases have identified a variety of abnormalities. These include alterations in neuronal morphology, excessive excitability, dysfunctional synaptic connections, and altered mitochondrial function, many that are likely to contribute to different disease phenotypes (Brennand and Gage, 2011; Brennand et al., 2011; Chiang et al., 2011; Devlin et al., 2015; Kim et al., 2011b; Liu et al., 2016; Robicsek et al., 2013; Sun et al., 2015; Sun et al., 2016). hiPSC-derived neuronal cultures can also serve as a valuable platform for evaluating the effect of a drug or drug combinations on gene-specific deficits in neuronal differentiation and/or function (Brennand et al., 2011; Marchetto et al., 2010). However, disease modeling *in vitro* with hiPSC-derived neurons is still at an early stage and there are a number of outstanding questions about the properties of neurons generated by a variety of differentiation protocols.

It is important that consistent criteria are used to define hiPSC-derived neurons in culture. Similar to criteria for characterizing induced neuronal (iN) cells reviewed by Yang et al., cells designated as neurons differentiated from hiPSCs should not only have neuronal morphology and express neuron specific markers, but should also be electrically excitable (Yang et al., 2011). In addition, the formation of functionally active synapses between neurons facilitates the use of cultures to explore how gene mutations potentially affect network activity. Second, there are a number of differentiation protocols used by different groups but little is known about the comparative efficiency with which these produce excitable cells (Maroof et al., 2013; Nicholas et al., 2013; Srikanth and Young-Pearse, 2014; Stover et al., 2013). In addition, it is not clear how the differentiation potentials of stem cells at different stages affect the formation of functionally active neurons. Some protocols incorporate the use of neural stem/progenitor cells, a self-renewing multipotent population derived from hiPSCs, as starting source for neuronal differentiation (Brafman, 2015; Stover et al., 2013; Yan et al., 2013). Other protocols start from the hiPSC stage, and directly differentiate cells into neurons without using an expandable population of multipotent cells (Devlin et al., 2015; Hartfield et al., 2014; Liu et al., 2013a; Liu et al., 2013b; Mertens, et al., 2015; Nicholas et al., 2013; Prè et al., 2014; Song et al., 2013; Sun et al., 2015; Zhang et al., 2013). Finally, when considering a single protocol there has been limited discussion of reproducibility in terms of the rate and degree of maturation of firing properties and synaptic connectivity between platings and between independently generated hiPSC lines. Low efficiency and/or high variability can hamper the identification of altered functional properties of neurons between control and mutant groups.

The goal of this study was to identify a protocol that could reliably produce cultures from hiPSCs in which the majority of cells with neuronal morphology also fire action potentials and form synaptic connections. The efficiency of generating functionally active neurons from one hiPSC line obtained from a control patient was evaluated using two different protocols. The first protocol included generating an expandable neuronal stem cell population that was plated onto astroglial feeder layers for differentiation. In our previous experience this resulted in cultures containing functionally active neurons but the efficiency was low (Brick et al., 2014; Stover et al., 2013). This was compared to a direct differentiation strategy that first patterns hiPSCs into neural progenitors (NPCs) that are differentiated without expansion (Liu et al., 2013a). The protocol was modified to include

the use of astroglial feeder layers for differentiation. Direct differentiation resulted in production of functionally active neurons at a faster rate and with higher efficiency than the protocol including an expandable intermediate population. In addition, the direct differentiation strategy resulted in cultures in which the rate and degree of neuronal maturation was similar between multiple platings from one control hiPSC line, and between two hiPSC lines from unrelated individuals with no known neurological disorders. hiPSC-derived neuronal cultures prepared using this direct differentiation will greatly facilitate identification of cellular defects in excitability and synaptic transmission associated with specific disease causing mutations and drug discovery.

2. Methods

2.1. Preparation and maintenance of hiPSCs

Two hiPSC cell lines, Line 210 (SC210.12-SF6-2I3.M11S8 through S31) and Line 173 (SC173.1-SF6-2I2.M16S9 through S21), were generated by the Schwartz laboratory using a previously published protocol (Stover et al., 2013) from skin fibroblasts provided by the labs of Alfred George, Jr. and Kevin Ess (210 line) and Philip Schwartz (173 line). Both control hiPSC lines maintained normal karyotype, and both fibroblast donors were males with no known clinical diagnoses. Age at time of biopsy was 23 years (210 line) and 56 years (173 line).

hiPSCs were maintained in feeder-free conditions using published protocols (Stover et al., 2013; Stover and Schwartz, 2011a). Briefly, hiPSCs were grown on Matrigel (BD Sciences, 354231) and fed every day with basal hiPSC medium supplemented with 2% (vol/vol) StemPro (StemPro SFM Kit, including 50× supplement, D-MEM/F12 + GlutaMax and 25% BSA solution, Life Technologies, A1000701) and 20 ng/ml bFGF (basic fibroblast growth factor, Stemgent, 03-0002). For basal medium, the final concentration of BSA and beta-mercaptoethanol (Life Technologies) in D-MEM/F12 + GlutaMax were 1.8% and 100 μM. Complete medium was equilibrated at 37 °C and 5% CO_2 before use.

hiPSCs were passaged upon reaching 100% confluence. Falcon 6-well plates were coated with a 1:30 dilution of Matrigel in D-MEM/F12 + Glutamax and incubated for at least 20 min. hiPSCs were incubated with 10 μm ROCK inhibitor (RI; rho-associated protein kinase inhibitor Y27632, Stemgent) 1 h prior to dissociation with Accutase (Millipore, SCR005) for 1 min at room temperature. Cells were dislodged and collected in Dulbecco's calcium- and magnesium-free phosphate-buffered saline (D-PBS; Gibco, 14190–144). The cell suspension was gently triturated, collected in conical tubes and centrifuged at 156 ×g for 5 min. Cell pellets were gently re-suspended in complete hiPSC medium plus RI. Excess Matrigel solution was removed from pre-incubated wells. The cell suspension was added to each well and then flooded with complete hiPSC media with RI to a final volume of 2 ml per well. Typical splits were from 1 well to 3 or 6 wells.

2.2. NSC culturing and neuronal differentiation

The 210 hiPSC line was also used to generate an expandable neural stem cell (exNSC 210) line. Line naming follows National Human Neural Stem Cell Resource nomenclature

(Stover et al., 2013). NSCs were maintained and passaged according to a previously published protocol (Stover et al., 2013) with no alterations. To prepare for neuronal differentiation, confluent NSC cultures were lifted using Enzyme Free Dissociation Buffer (Life Technologies, 13150-016), dislodged, and collected using D-PBS. The cell suspension was then gently triturated, collected in conical tubes and centrifuged at 156 $\times g$ for 5 min. After re-suspension in fresh NSC media (see published protocol) cell suspension was passed through a 37 μm reversible strainer (STEMCELL Technologies, 27215). This revised step to the protocol removes the large non-dissociated clusters of NSCs and allows plating of single cells on 50% confluent mouse glia at a density 2.2×10^4 cells/cm^2 per coverslip. Neuronal differentiation was also performed as per the original protocol, but with the addition of 0.2 μM γ-secretase inhibitor XXI (Compound E; Calbiochem, 565790) during the first 3 days of differentiation. Neuronal differentiation media contained 20 ng/ml BDNF (Peprotech, 450-02), GDNF (Peprotech, 450-10), 1 mM dibutyryl cAMP (Sigma-Aldrich, D0260), and 200 nM freshly made ascorbic acid (Sigma-Aldrich, A403). Feeding cultures involved a 50% exchange every 48 h for the duration of the culture's life. All media was prepared immediately prior to use and equilibrated at 37 °C and 5% CO_2.

2.3. Direct differentiation of hiPSCs into neurons

The strategy used to pattern hiPSCs into neurons was adapted from a previously published protocol (Liu et al., 2013a). On day 0, embryoid bodies were generated from 100% confluent hiPSC cultures grown in a 6-well falcon plate by manual scraping in a parallel direction using a 1 ml pipette tip. Tissue fragments from 15 wells were collected in a conical tube. After centrifugation at 156 $\times g$ for 5 min the pellet was re-suspended in 15 ml hiPSCM (human hiPSC medium) and then transferred to a T25 non-tissue culture treated flask (Thermofisher Scientific, 169900). Neural induction and culturing protocols were followed as per the original protocol. On day 16, neural rosettes were collected using STEMDiff Neural Rosette Selection reagent (STEMCELL Technologies, 05832) based on vendor's protocol. MGE patterning was done using the ventralizing factors purmorphamine (Stemgent, 04-0009) and/or recombinant human sonic hedgehog (SHH; Peprotech) following the original protocol until day 25. Experiments using purmorphamine with SHH and purmorphamine alone were included in this study.

Neuronal differentiation was initiated on day 26, when progenitor neurospheres were dissociated using Accutase, centrifuged at 156 $\times g$ for 5 min, and re-suspended in neural induction medium (NIM) containing Rho kinase (ROCK) inhibitor. These were plated at 2.2×10^4 cells/cm^2 per coverslip on 50% confluent mouse astroglial cultures. 24 h after plating, 50% of the NIM was replaced with complete NDM (Neural differentiation medium) containing 0.4 μM Compound E, 10 ng/ml BDNF, 10 ng/ml GDNF, 10 ng/ml IGF-1 (Peprotech, 100-11), and 0.5 g/ml membrane permeable cyclic AMP. 48 h after plating, all of the culture medium was replaced by complete NDM supplemented with 0.2 μM Compound E. 96 h after plating, culture medium was replaced with complete NDM and a 50% exchange with fresh complete NDM performed every 48 h for the duration of the culture's life. All media was prepared immediately prior to use and equilibrated at 37 °C and 5% CO_2.

2.4. Astroglial cultures

Astroglial cultures were generated using a previously published protocol (Hilgenberg and Smith, 2007; Schutte et al., 2017). Briefly, cortical rinds were dissected from the brains of P0–P2 ICR (CD-1) mouse pups (Envigo), enzymatically digested, and triturated into a single cell suspension. Suspension was plated on poly-D-lysine (PDL, Sigma-Aldrich, P7886) coated 60 mm tissue culture dishes and allowed to grow to confluence. Once confluent, cultures were trypsinized (TrypLE, Life Technologies, 12604-021), lifted, re-suspended in freezing media (Glia Culture Medium with 10% DMSO) and stored at −80 °C. When needed, cells were defrosted and 4.4×10^4 cells/cm^2 per coverslip viable (identified by trypan blue staining) cells/cm^2 were plated onto PDL-coated 12 mm glass coverslips (Bellco Glass, 1943-10012A). Astroglial feeder cultures were grown for 5–6 days to approximately 50% visually determined confluence prior to seeding with neural progenitors for neuronal differentiation.

2.5. Immunostaining and imaging

Coverslips containing hiPSC- or exNSC-derived neurons were fixed in 4% paraformaldehyde (in PBS, Sigma-Aldrich, P6148) for 15 min at room temperature and washed three times with PBS. Cells were permeabilized and blocked using PBS with 4% bovine serum albumin (wt/vol) (BSA; Sigma-Aldrich, A4919), 0.25% Triton X-100 (vol/vol) (Sigma-Aldrich, X100), and 0.02% sodium azide (wt/vol) (Sigma-Aldrich, S2002) in 1× PBS (Sigma-Aldrich, P3813) for 1 h at room temperature. Cultures were exposed to primary antibody and incubated overnight at 4 °C. After washing 3 times with PBS, coverslips incubated in 5% normal goat serum (vol/vol) (ThermoFisher Scientific, 16210-064), 0.25% Triton X-100, 0.02% sodium azide (wt/vol) in 1× PBS containing a 1:1000 dilution of secondary antibody (Alexa-Fluor; Life Technologies) for 2 h at room temperature. Coverslips were washed twice with PBS before staining nuclei with 4′,6-diamidino-2-phenylindole (DAPI; Life Technologies, D9542). Fluoromount G (SouthernBiotech, 0100-01) was used to mount coverslips on glass slides. Images were taken using a Zeiss M2 Imager microscope and processed by Zen software. HuNu (1:250; Millipore, MAB1281), βIII-tubulin (1:2000; BioLegend, 802001) and GFAP (glial fibrillary acidic protein; 1:1500; DAKO, Z0334) were used to characterize composition of cells generated from hiPSCs by the direct differentiation protocol. βIII-tubulin (Sigma-Aldrich, T8660) and GABA (Sigma-Aldrich, A2052) primary antibodies were used at 1:1000 and 1:4000 dilutions respectively for identification of GABAergic neurons. Neurons were identified by morphology, expression of βIII-tubulin in the soma and neurites, and nuclear localization of DAPI.

2.6. Whole-cell recording

Whole cell recordings were obtained from hiPSC-derived neurons at 5 different time points: 4–5, 10–11, 15–16, 21–23, and 35–38 days post plating. exNSC-derived neurons were examined at 21–23 days post plating. Electrophysiological recordings were performed with unpolished borosilicate glass pipettes with open tip resistance of 4–7 MΩ (VWR International, 53432-921). External solution contained (in mM): NaCl 120, KCl 5.4, MgCl$_2$ 0.8, CaCl$_2$ 1.8, glucose 15, HEPES 20, at pH 7.2–7.4. Osmolality was adjusted to 290–295

mOsm. Internal solution contained (in mM): potassium gluconate 120, NaCl 20, $CaCl_2$ 0.1, $MgCl_2$ 2, EGTA 1.1, HEPES 10, Na_2ATP 4.5 with pH at 7.2 and osmolality around 280 mOsm. Voltages were corrected for a – 5 mV junction potential. Spontaneous action potential firing was recorded both at resting membrane potential and at –75 mV using a gap free protocol under current clamp. For evoked action potentials, membrane potential was held at –75 mV and cells were depolarized by a series of current injections. Spontaneous postsynaptic currents (sPSCs) were examined under voltage clamp at –75 mV.

Spontaneous excitatory and inhibitory postsynaptic currents (sEPSCs and sIPSCs) were separated at reversal potentials (–49 mV and –2 mV) with the same external solution mentioned above and CsGluconate internal solution containing (in mM): Cs^+ gluconate 130, EGTA 0.2, $MgCl_2$ 2, CsCl 6, HEPES 10, adenosine 5′ triphosphate sodium salt 2.5, guanosine 5′ triphosphate sodium 0.5 and phosphocreatine disodium 10. The identity of sEPSCs and sIPSCs were confirmed pharmacologically using 50 μM (2*R*)-amino-5-phosphonovaleric acid (APV; Tocris Bioscience, 0106), 10 μM 6-cyano-7-nitroquinoxaline-2,3-dione (CNQX; Sigma-Aldrich, C127), 10 μM bicuculline methochloride (BMC; Tocris Bioscience, 0131), and/or 100 nM strychnine (Sigma-Aldrich, S8753) bath applied in external solution. External solution was perfused through the chamber at a speed of 0.6 to 1 ml/min during recording.

2.7. Data analysis and statistics

Fluorescent micrographs processed using Zen software were used to quantify the percentage of GABAergic neurons. For each coverslip, at least 3 fields with equally distributed cells observed *via* DIC were chosen for counting. Counting was performed blind with respect to cell line. Represented data were based on n = 10 coverslips (Line 210) and n = 4 coverslips (Line 173).

Electrophysiological data were acquired with a List EPC7 amplifier, a Digidata 1320A D-A converter (Axon Instruments), and a Dell Optiplex GX110 computer running pClamp8 (Axon Instruments) software at room temperature. Clampfit 10.6 software (Axon Instruments) was used to analyze electrophysiological data.

Cells that were included in analyses had an input resistance   400 MΩ, whole-cell capacitance   5 pF, stable (no greater than a ± 5 mV deviation) resting membrane potentials more hyperpolarized than –30 mV, and stable sPSC voltage-clamp recordings. We characterized evoked action potentials as regenerative events with a peak depolarization of greater than or equal to –5 mV on the first AP and –15 mV in subsequent APs within the train. sPSCs recorded under voltage-clamp were analyzed using Mini Analysis 6.0.7 (Synaptosoft). sPSCs identified by the software had an amplitude   10 pA (2× RMS noise of 2.5 pA) and were then manually verified individually. sPSC recordings in which the baseline shifted by >50 pA were excluded. Electrophysiological data were represented based on n = number of independent experiments. All statistical analyses were performed with Prism 7.0.2 (GraphPad Software) and all figures were generated using DeltaGraph 7.1 (Red Rock Software).

3. Results

3.1. hiPSCs-derived neurons mature more rapidly than those generated from an expandable NSC intermediate stage

Our initial studies focused on the comparison of neurons derived using two different protocols from the same human control hiPSC line (Line 210) (Fig. 1A). The first protocol involved generating an expandable population of neural stem cells (exNSCs) from the hiPSCs (Fig. 1B, top) (modified from Stover et al., 2013). The exNSCs were maintained as a renewable population and plated at a density of 2.2×10^4 cells/cm^2 onto 50% confluent mouse astrocyte-enriched feeder layers to begin differentiation (D0) into exNSC-neurons. The second protocol was based on patterning hiPSCs into neural progenitor cells (NPCs) over a period of 26 days followed by immediate plating at a density of 2.2×10^4 cells/cm^2 onto the astrocyte-enriched feeder layers to begin differentiation (D0) into hiPSC-derived neurons (Fig. 1B, bottom). By the 3rd week of differentiation (D21–23 post plating), cultures prepared using both protocols contained cells with neurites that also expressed the neuron specific marker βIII-tubulin (Fig. 1C, top). The cultures generated *via* direct differentiation typically had a more extensive network of branched neurites compared to cultures generated through an exNSC intermediate stage (Fig. 1C, bottom).

Electrical excitability following 21 days of differentiation was compared in neurons derived using the two protocols. The typical exNSC-neuron displayed passive changes in membrane potential or small failed spikes in response to depolarizing current injection (Fig. 1D, top). In contrast, the typical hiPSC-derived neuron fired multiple action potentials in response to stimulation (Fig. 1D, bottom). Evaluation of over 20 neurons using the two protocols demonstrated a significantly higher percentage of hiPSC-derived neurons firing at least one action potential (AP) in response to a depolarizing current injection compared to exNSC-neurons ($p < 0.0001$; Chi-square test; Fig. 1E). These data demonstrate that the rate of maturation of excitability is faster in neurons generated by the direct differentiation protocol compared to those generated from an expandable NSC intermediate stage.

Consistent with more extensive neuritic arbors, the average whole-cell capacitance (C_m) of the hiPSC-derived neurons generated *via* direct differentiation was 2.5 times larger than in exNSC-neurons (Table 1). However, there was no significant difference in the input resistance (R_{in}) or resting membrane potential (RMP) between neurons generated from the two protocols at D21 post plating (Table 1, $p > 0.2$, unpaired *t*-test with Welch's correction).

3.2. Direct differentiation protocol produces primarily neurons

Since the direct differentiation protocol results in a faster maturation of functionally active neurons than the exNSC protocol, the remainder of this work focuses on cultures prepared by direct differentiation. To determine if the hiPSCs give rise to astroglial cells as well as neurons, we prepared cultures from the 210 line and from a second hiPSC control line (173) from an unrelated donor with no known neurological disorders. Cultures were fixed and immunostained at 3 weeks post plating. As hiPSC-derived NPCs are plated onto astrocyte feeder layers of mouse origin, human derived cells were identified by immunostaining with HuNu, a marker for human nuclei. HuNu positive cells that were also positive for the

neuronal maker βIII-tubulin had classic neuronal morphology with branched neuritic processes and cell bodies that appeared to have volume in DIC optics (white arrows indicate the cell body of one neuron on both the overlay panel and the DIC panel for each cell line in Fig. 2A). There was also a small population of cells with irregularly shaped, flattened cell bodies that expressed HuNu but were not βIII-tubulin positive (light blue arrowhead indicates one non-neuronal cell, on overlay panel and DIC panel for each cell line in Fig. 2A). When cultures were immunostained with antibodies of HuNu and GFAP, a small population of flattened, irregularly shaped cells were positive for both, identifying these as hiPSC derived astroglia (orange arrowhead indicates one astroglial cell for each cell line in Fig. 2C). The mouse astroglial cells in the feeder layer were identified as the DAPI positive, HuNu negative cells stained with GFAP. Quantitative analysis on 3 individual coverslips from 2 independent platings from both control lines revealed 98% of the human-derived cells were neurons and 2% were astroglia ($p > 0.75$, unpaired t-test with Welch's correction, Fig. 2B and D). These data demonstrate that two independent control lines both give rise to predominantly neurons using the direct differentiation protocol.

3.3. Intrinsic firing properties of hiPSC-derived neurons evaluated in multiple platings from two independent control hiPSC lines

To evaluate the rate of neuronal maturation and determine if this is consistent across multiple platings from one hiPSC line and between different hiPSC lines, we generated neuronal cultures prepared from two control hiPSC lines (210 and 173) using the direct differentiation protocol. Multiple independent platings of each hiPSC line were evaluated over the course of 5 weeks post plating. All firing properties are presented as averages from 4 or more platings, with n representing the number of platings. There were 5 or more individual neurons examined in each plating at each time point.

Cultures from both lines contained cells with βIII-tubulin positive neurites and the degree of neurite complexity increased with time in culture (Fig. 3A). The cultures also contained cells that fired action potentials in response to depolarizing current injections as early as D4–5 post plating and at each time point examined up through D35–38 post plating (Fig. 3B). Quantitative analysis of evoked firing focused on three properties: the percentage of cells capable of firing at least one AP (Fig. 3C), percentage of cells firing repetitively (2 or more APs) (Fig. 3D) and the average peak evoked firing frequency (Fig. 3E). There was a significant increase in all three properties as a function of time in culture in both cell lines (age effect: $p < 0.0001$; two-way ANOVA; Figs. 3C–E). The variance between plating was the lowest for the percentage of cells firing at least one AP as evidenced by the smaller error bar representing standard deviation (Fig. 3C). The highest variance between platings was seen in percentage of cells firing repetitively and firing frequencies, most prominently at the intermediate time periods between D10 and D23 post plating (Fig. 3D and E). However, there was no difference in any of these properties between the control lines (cell line effect: $p > 0.98$, $p > 0.10$, $p > 0.17$, respectively; Figs. 3C–E; Table 3).

Taken together, these data demonstrate that the direct differentiation protocol reliably produces cultures from hiPSCs in which a high percentage of cells with neuronal

morphology are electrically excitable, and the rate of maturation of firing properties is similar from plating to plating.

3.4. Formation of spontaneously active networks of excitatory and inhibitory cells

Neurons in both the control 210 and 173 cultures exhibited spontaneous firing patterns that were classified as irregular tonic firing with single spikes (Fig. 4Ai and 4Aii) or burst firing (2 sAPs within a single depolarization) (Fig. 4Aiii and 4Aiv). In the absence of applied holding current a small percentage of hiPSC-derived neurons from both lines fired spontaneously in one of the two patterns as early as D4–5 post plating and this increased significantly as a function of age in culture ($p < 0.0001$; two-way ANOVA with *post hoc* Bonferroni test; Fig. 4B). In the control 210 cultures, the percentage of hiPSC-derived neurons firing spontaneously continued to increase steadily until D35–38. In contrast, in the control 173 derived neurons, there was no further increase in the percentage of cell firing spontaneously beyond D15–16, and this property was significantly different between the two control lines at the later time points (age effect: $p < 0.0001$; two-way ANOVA; Fig. 4B; Table 3). About half of the spontaneously firing cells were spontaneously burst firing in both lines. The percentage of cells exhibiting burst firing significantly increased with age ($p < 0.001$; two-way ANOVA) and there was no significant difference between lines (cell line effect: $p > 0.63$; two-way ANOVA with *post hoc* Bonferroni test; Fig. 4C; Table 3). When compared to evoked firing, spontaneous firing was marked by greater variability between platings within each line, indicated by larger standard deviations.

Spontaneous synaptic activity was also observed in neurons derived from both control hiPSC lines (Fig. 5A). To quantify the degree of synaptic connectivity, the percentage of neurons with spontaneous postsynaptic potentials (sPSP) or postsynaptic currents (sPSCs) was determined at a holding potential of −75 mV. Over 40% of cells from both control hiPSC lines had detectable sPSP and/or sPSCs at the earliest time point, D4 post plating (Fig. 5B). Assessment of the sPSC frequency demonstrated a steady and significant increase from 0.02 Hz for D4–5 cells to a mean of 4–5 Hz by D35–38 post plating (age effect: $p < 0.001$; two-way ANOVA with *post hoc* Bonferroni test; Fig. 5C). The variance in this property between platings became larger over time, with the greatest variance at D35–38 post plating when the sPSC frequencies ranged from 1 to 13 Hz. There was no significant difference between the control lines in the percentage of cells with spontaneous synaptic input or the sPSC/P frequency (cell line effect: $p > 0.13$ and $p > 0.85$, respectively; two-way ANOVA with *post hoc* Bonferroni test; Fig. 5B and C).

A subpopulation of neurons derived from control hiPSC line 210 and 173 was examined to determine the identity of the receptors mediating synaptic transmission. At the reversal potential for chloride mediated currents (−49 mV), all of the fast decaying currents were completely blocked by 50 μM APV and 10 μM CNQX, indicating they were spontaneous excitatory postsynaptic currents (sEPSC) mediated by AMPA and NMDA receptors (Fig. 5D). At the reversal potential for glutamatergic currents (−2 mV), the large majority of slow decaying currents were blocked by a $GABA_A$ receptor antagonist BMC in 10 μM. A small percentage was insensitive to BMC, but could be blocked by an antagonist of glycine receptors strychnine in 100 nM (Fig. 5D). This suggests the cultures from both lines contain

a predominantly glutamatergic neurons and GABAergic neurons, and a small proportion of glycinergic neurons. Over 75% of neurons derived from hiPSC lines 210 and 173 received both excitatory and inhibitory synaptic input at day 21–23 post plating, demonstrating a functional neural network with both excitation and inhibition (p = 0.16, Chi-square test; Fig. 5E).

There was a steady decrease in input resistance over time between 2 and 5 weeks in culture, and this property was similar between the two lines (Table 2). In both the 210 and 173 hiPSC-derived neurons the mean whole cell capacitance increased steadily over time and there was no change in the resting membrane potential (C_m age effect: p < 0.0001; RMP age effect: p > 0.18; two-way ANOVA with *post hoc* Bonferroni test; Table 2; Table 3). Although a two-way ANOVA identified that the resting membrane potential was slightly more hyperpolarized in 210 compared to 173 (cell line effect: p < 0.05; two-way ANOVA); subsequent *post hoc* analyses were unable to resolve any significant time points between lines (Table 2; Table 3). The whole cell capacitance was larger in 210 cells (cell line effect: p < 0.0001; two-way ANOVA with *post hoc* Bonferroni test), and this was significant at D15–16 and D21–24 post plating (Table 2; Table 3). Overall, these data demonstrate that the direct differentiation protocol results in a rate and degree of maturation in excitability and synaptic transmission that is consistent from plating to plating, and similar for most properties examined between two different control hiPSC lines.

3.5. Identification of GABAergic neurons

The observation of both glutamatergic and GABAergic synaptic currents indicated that, despite the use of ventralizing factors, our protocol supports differentiation of both excitatory and inhibitory neurons. To quantify the percentage of total hiPSC-derived neurons that are GABAergic, cultures were fixed at D21–23 and stained with anti-βIII-tubulin and anti-GABA antibodies (Fig. 6A). Approximately 30% of the neurons were GABA positive, and there was no significant difference in the percent of total neurons that were GABA positive in the 210 and 173 hiPSC-derived neuronal cultures (p > 0.14, unpaired *t*-test with Welch's correction; Fig. 6B). These data, in conjunction with the synaptic current recordings, confirm that our direct differentiation protocol produced mixed cultures with both inhibitory GABAeric and excitatory glutamatergic neurons.

4. Discussion

4.1. Difference in maturation of excitability in expandable intermediate population vs direct differentiation

In our study, neurons generated by the direct differentiation protocol were more electrically excitable than the expandable NSC-derived neurons over the first 5 weeks of neuronal differentiation. From previous studies in our lab we know that neurons in cultures from expandable NSCs at later times are able to develop repetitive firing properties (Stover et al., 2013). Another study using expandable NPC-derived neurons also reported an extended timeline of maturation, with the large majority of the cells capable of firing multiple action potentials in NPC cultures by 6 weeks post plating (Tang et al., 2013). Therefore, it is likely that at least some of the difference between the expandable NSC or NPC strategy *versus* the

direct differentiation protocol is the rate as opposed to capacity for maturation. A recent study predicting functional states of expandable NPC-derived neurons with RNA-seq and electrophysiology reports a decline in degree of maturation with increased passage number of the intermediate population (Bardy et al., 2016). However, by day 30 post plating, the differentiation of excitability and synaptic activity in the neurons was similar to neurons generated by the direct differentiation in the present paper. Enhanced neuronal function observed in the Bardy study may be due to the BrainPhys growth medium that has been shown to support action potential firing and synaptic transmission in hiPSC-derived neurons (Bardy et al., 2015). Future studies will be important to determine if the BrainPhys medium can further increase the rate and/or the degree of maturation in directly differentiated neurons.

4.2. Reproducibility in rate/degree of functional maturation between platings and between hiPSC lines

The direct differentiation protocol results in a high percentage of functionally active cells in each plating from two different hiPSC lines. However, there were differences in the degrees of variance and in the rate of maturation between properties. In general, hiPSC-derived neurons from both lines exhibited a lower degree of variability in evoked firing *vs* spontaneous activity at each time point. This suggests that, in order to identify functional changes associated with a specific mutation, the direct differentiation protocol is better suited to resolving differences in intrinsic excitability, and small differences in spontaneous firing or synaptic transmission will require a larger number of trials to establish significance (Devlin et al., 2015; Hu et al., 2010; Kim et al., 2011a; Liu et al., 2016).

The control lines in the present study were from donors of different ages, 23 and 56. The similarly high percentage of neurons to glial cells derived from both hiPSCs lines in the direct differentiation protocol suggest donor age does not affect the efficiency of producing neuronal cells. This is consistent with a previous study using a different differentiation protocol demonstrating donor age did not influence the percentage of hiPSC-derived cells positive for ISL, a motor neuron marker (Boulting et al., 2011). In addition, while donor age does not appear to influence the rate/degree of the majority of functional properties examined, we cannot rule out the possibility that donor age affects the two properties that were different between the lines: maturation of the percentage of cells firing spontaneous action potentials and resting membrane potential. It would be interesting to systematically study the effect of age on functional development of neurons using multiple iPSCs lines.

Whole-cell capacitance increased steadily as a function of age in neurons derived from both cell lines. However, while the 173 *vs* the 210 derived neurons had a smaller capacitance at each time point, indicative of lower total membrane surface area, the differentiation of functional properties was comparable. This indicates that cell size in this case is not highly correlated with functional differentiation. In addition, the difference in whole cell capacitance does not appear to be a property of the specific hiPSC cell line because a set of neurons derived from the 173 line in our previous study had capacitance values similar to those of the 210 line in the current study (Schutte et al., 2017). One possibility is that a variance in the size of embryoid bodies and neurospheres during the initial phase of

patterning could affect exposure to morphogens and result in variance in the starting cell size. This could be further examined using Aggrewell™ plating methods to control the size of embryoid bodies by plating a similar amount of dissociated cells into pocket-like microwells (Stover and Schwartz, 2011b).

4.3. Neuronal subtypes in culture

The ability to generate well-defined populations of excitatory or inhibitory neurons is an important prerequisite for use of pluripotent stem cells in human transplantation studies. A recent study demonstrated that exposure to different levels of purmorphamine can produce nearly pure yields of glutamatergic, GABAergic, or medium spiny neurons (Yuan et al., 2015). Having precise control over the terminal phenotype of grafted cells bypasses concerns of unintended integration of other subtypes and can balance excitatory and inhibitory neuronal network activity in the recipient (Cunningham et al., 2014; Fortin et al., 2016; Hunt et al., 2013). Therefore it was surprising that only 30–40% of the neurons generated in the direct differentiation protocol were GABAergic, using a concentration of SMAD inhibitors and purmorphamine that in other similar protocols yielded cultures in which 80–90% of the neurons were GABAergic (Liu et al., 2013a; Nicholas et al., 2013; Yuan et al., 2015). This difference could have arisen from variations in the size of embryoid bodies and neuroepithethelial tissue generated during the patterning process, in which the generation of distinct morphogen gradients may contribute to regional specification of neurons (Suzuki and Vanderhaeghen, 2015). Another difference could have arisen from the use of mouse astroglial feeder layers for the differentiation phase in the present study. Previous studies have shown that astrocytes are important for regulating the microenvironment of differentiating neurons through cell-cell contact and secreted factors (Berg et al., 2013; Chung et al., 2015).

There are important advantages in having mixed cultures of excitatory and inhibitory neurons for disease modeling. First, the mix of functional glutamatergic and GABAergic neurons more accurately reflects a native neural network, with the number of excitatory cells outnumbering GABAergic. Second, both excitatory and inhibitory inputs are essential for maintaining a stable E/I ratio in neurons, which play an important role in cortical functions in mammalian cerebral cortex (Xue et al., 2014). Imbalance of E/I is associated with epilepsy, autism and fragile X syndrome (Gibson et al., 2008; Nelson and Valakh, 2015). Therefore, generating neuronal cultures with both excitatory and inhibitory neurons, instead of pure population of certain cell types, facilitates understanding in the altered relationship of E/I in the disease models *in vitro*.

In conclusion, direct differentiation of neurons from hiPSC lines resulted in the reproducible and efficient generation of electrophysiologically active neuronal cultures from independent donors. The establishment of baseline parameters concerning the development and maturation of derived neurons is critical for interpretation of data obtained using this rapidly evolving platform. In particular, for investigations utilizing non-isogenic iPSC lines from affected individuals and related (or unrelated) controls, a quantitative characterization of electrophysical properties and their variation resulting from the selected differentiation protocol is required. The functional outcomes of the differentiation protocol utilized in this

study establishes a platform for the identification of mutational or drug-induced functional alternations, which is at the core of preclinical disease modeling.

Acknowledgments

References

Bardy C, van den Hurk M, Eames T, Marchand C, Hernandez RV, Kellogg M, Gorris M, Galet B, Palomares V, Brown J, Bang AG, Mertens J, Bohnke L, Boyer L, Simon S, Gage FH. Neuronal medium that supports basic synaptic functions and activity of human neurons in vitro. Proc Natl Acad Sci U S A. 2015; 112:E2725–2734. [PubMed: 25870293]

Bardy C, van den Hurk M, Kakaradov B, Erwin JA, Jaeger BN, Hernandez RV, Eames T, Paucar AA, Gorris M, Marchand C, Jappelli R, Barron J, Bryant AK, Kellogg M, Lasken RS, Rutten BP, Steinbusch HW, Yeo GW, Gage FH. Predicting the functional states of human iPSC-derived neurons with single-cell RNA-seq and electrophysiology. Mol Psychiatry. 2016; 21:1573–1588. [PubMed: 27698428]

Berg DA, Belnoue L, Song H, Simon A. Neurotransmitter-mediated control of neurogenesis in the adult vertebrate brain. Development. 2013; 140:2548–2561. [PubMed: 23715548]

Boulting GL, Kiskinis E, Croft GF, Amoroso MW, Oakley DH, Wainger BJ, Williams DJ, Kahler DJ, Yamaki M, Davidow L, Rodolfa CT, Dimos JT, Mikkilineni S, MacDermott AB, Woolf CJ, Henderson CE, Wichterle H, Eggan K. A functionally characterized test set of human induced pluripotent stem cells. Nat Biotechnol. 2011; 29:279–286. [PubMed: 21293464]

Brafman DA. Generation, expansion, and differentiation of human pluripotent stem cell (hPSC) derived neural progenitor cells (NPCs). Methods Mol Biol. 2015; 1212:87–102. [PubMed: 25063499]

Brennand KJ, Gage FH. Concise review: the promise of human induced pluripotent stem cell-based studies of schizophrenia. Stem Cells. 2011; 29:1915–1922. [PubMed: 22009633]

Brennand KJ, Simone A, Jou J, Gelboin-Burkhart C, Tran N, Sangar S, Li Y, Mu Y, Chen G, Yu D, McCarthy S, Sebat J, Gage FH. Modelling schizophrenia using human induced pluripotent stem cells. Nature. 2011; 473:221–225. [PubMed: 21490598]

Brick DJ, Nethercott HE, Montesano S, Banuelos MG, Stover AE, Schutte SS, O'Dowd DK, Hagerman RJ, Ono M, Hessl DR, Tassone F, Schwartz PH. The autism Spectrum disorders stem cell resource at Children's Hospital of Orange County: implications for disease modeling and drug discovery. Stem Cells Transl Med. 2014; 3:1275–1286. [PubMed: 25273538]

Chiang CH, Su Y, Wen Z, Yoritomo N, Ross CA, Margolis RL, Song H, Ming GL. Integration-free induced pluripotent stem cells derived from schizophrenia patients with a DISC1 mutation. Mol Psychiatry. 2011; 16:358–360. [PubMed: 21339753]

Chung WS, Allen NJ, Eroglu C. Astrocytes control synapse formation, function, and elimination. Cold Spring Harb Perspect Biol. 2015; 7:a020370. [PubMed: 25663667]

Cunningham M, Cho JH, Leung A, Savvidis G, Ahn S, Moon M, Lee PKJ, Han JJ, Azimi N, Kim KS, Bolshakov VY, Chung S. Human PSC-derived maturing GABAergic interneurons ameliorate seizures and abnormal behavior in epileptic mice. Cell Stem Cell. 2014; 15:559–573. [PubMed: 25517465]

Devlin AC, Burr K, Borooah S, Foster JD, Cleary EM, Geti I, Vallier L, Shaw CE, Chandran S, Miles GB. Human iPSC-derived motoneurons harbouring TARDBP or C9ORF72 ALS mutations are dysfunctional despite maintaining viability. Nat Commun. 2015; 6:5999. [PubMed: 25580746]

Fortin JM, Azari H, Zheng T, Darioosh RP, Schmoll ME, Vedam-Mai V, Deleyrolle LP, Reynolds BA. Transplantation of defined populations of differentiated human neural stem cell progeny. Sci Rep. 2016; 6:23579. [PubMed: 27030542]

Gibson JR, Bartley AF, Hays SA, Huber KM. Imbalance of neocortical excitation and inhibition and altered UP states reflect network hyperexcitability in the mouse model of fragile X syndrome. J Neurophysiol. 2008; 100:2615–2626. [PubMed: 18784272]

Hartfield EM, Yamasaki-Mann M, Ribeiro Fernandes HJ, Vowles J, James WS, Cowley SA, Wade-Martins R. Physiological characterisation of human iPS-derived dopaminergic neurons. PLoS One. 2014; 9:e87388. [PubMed: 24586273]

Hilgenberg LGW, Smith MA. Preparation of dissociated mouse cortical neuron cultures. J Vis Exp. 2007:562. [PubMed: 18989405]

Hu BY, Weick JP, Yu J, Ma LX, Zhang XQ, Thomson JA, Zhang SC. Neural differentiation of human induced pluripotent stem cells follows developmental principles but with variable potency. Proc Natl Acad Sci U S A. 2010; 107:4335–4340. [PubMed: 20160098]

Hunt RF, Girskis KM, Rubenstein JL, Alvarez-Buylla A, Baraban SC. GABA progenitors grafted into the adult epileptic brain control seizures and abnormal behavior. Nat Neurosci. 2013; 16:692–697. [PubMed: 23644485]

Kim JE, O'Sullivan ML, Sanchez CA, Hwang M, Israel MA, Brennand K, Deerinck TJ, Goldstein LSB, Gage FH, Ellisman MH, Ghosh A. Investigating synapse formation and function using human pluripotent stem cell-derived neurons. Proc Natl Acad Sci U S A. 2011a; 108:3005–3010. [PubMed: 21278334]

Kim KY, Hysolli E, Park IH. Neuronal maturation defect in induced pluripotent stem cells from patients with Rett syndrome. Proc Natl Acad Sci U S A. 2011b; 108:14169–14174. [PubMed: 21807996]

Liu Y, Liu H, Sauvey C, Yao L, Zarnowska ED, Zhang SC. Directed differentiation of forebrain GABA interneurons from human pluripotent stem cells. Nat Protoc. 2013a; 8:1670–1679. [PubMed: 23928500]

Liu Y, Lopez-Santiago LF, Yuan Y, Jones JM, Zhang H, O'Malley HA, Patino GA, O'Brien JE, Rusconi R, Gupta A, Thompson RC, Natowicz MR, Meisler MH, Isom LL, Parent JM. Dravet syndrome patient-derived neurons suggest a novel epilepsy mechanism. Ann Neurol. 2013b; 74:128–139. [PubMed: 23821540]

Liu J, Gao C, Chen W, Ma W, Li X, Shi Y, Zhang H, Zhang L, Long Y, Xu H, Guo X, Deng S, Yan X, Yu D, Pan G, Chen Y, Lai L, Liao W, Li Z. CRISPR/Cas9 facilitates investigation of neural circuit disease using human iPSCs: mechanism of epilepsy caused by an SCN1A loss-of-function mutation. Transl Psychiatry. 2016; 6:e703. [PubMed: 26731440]

Marchetto MC, Carromeu C, Acab A, Yu D, Yeo GW, Mu Y, Chen G, Gage FH, Muotri AR. A model for neural development and treatment of Rett syndrome using human induced pluripotent stem cells. Cell. 2010; 143:527–539. [PubMed: 21074045]

Maroof AM, Keros S, Tyson JA, Ying SW, Ganat YM, Merkle FT, Liu B, Goulburn A, Stanley EG, Elefanty AG, Widmer HR, Eggan K, Goldstein PA, Anderson SA, Studer L. Directed differentiation and functional maturation of cortical inter-neurons from human embryonic stem cells. Cell Stem Cell. 2013; 12:559–572. [PubMed: 23642365]

Mertens J, Wang QW, Kim Y, Yu DX, Pham S, Yang B, Zheng Y, Diffenderfer KE, Zhang J, Soltani S, Eames T, Schafer ST, Boyer L, Marchetto MC, Nurnberger JI, Calabrese JR, Ødegaard KJ, McCarthy MJ, Zandi PP, Alba M, Nievergelt CM, Mi S, Brennand KJ, Kelsoe JR, Gage FH, Yao J. The Pharmacogenomics of Bipolar Disorder. Differential responses to lithium in hyperexcitable neurons from patients with bipolar disorder. Nature. 2015; 527:95–99. [PubMed: 26524527]

Nelson, Sacha B., Valakh, V. Excitatory/inhibitory balance and circuit homeostasis in autism Spectrum disorders. Neuron. 2015; 87:684–698. [PubMed: 26291155]

Nicholas CR, Chen J, Tang Y, Southwell DG, Chalmers N, Vogt D, Arnold CM, Chen YJ, Stanley EG, Elefanty AG, Sasai Y, Alvarez-Buylla A, Rubenstein JL, Kriegstein AR. Functional maturation of hPSC-derived forebrain interneurons requires an extended timeline and mimics human neural development. Cell Stem Cell. 2013; 12:573–586. [PubMed: 23642366]

Prè D, Nestor MW, Sproul AA, Jacob S, Koppensteiner P, Chinchalongporn V, Zimmer M, Yamamoto A, Noggle SA, Arancio O. A time course analysis of the electrophysiological properties of neurons differentiated from human induced pluripotent stem cells (iPSCs). PLoS One. 2014; 9:e103418. [PubMed: 25072157]

Robicsek O, Karry R, Petit I, Salman-Kesner N, Muller FJ, Klein E, Aberdam D, Ben-Shachar D. Abnormal neuronal differentiation and mitochondrial dysfunction in hair follicle-derived induced pluripotent stem cells of schizophrenia patients. Mol Psychiatry. 2013; 18:1067–1076. [PubMed: 23732879]

Schutte RJ, Xie Y, Ng NN, Figueroa P, Pham AT, O'Dowd DK. Astrocyte-enriched feeder layers from cryopreserved cells support differentiation of spontaneously active networks of human iPSC-derived neurons. J Neurosci Methods. 2017; 294:91–101. [PubMed: 28746822]

Song M, Mohamad O, Chen D, Yu SP. Coordinated development of voltage-gated Na+ and K+ currents regulates functional maturation of forebrain neurons derived from human induced pluripotent stem cells. Stem Cells Dev. 2013; 22:1551–1563. [PubMed: 23259973]

Srikanth P, Young-Pearse TL. Stem cells on the brain: modeling neurodevelopmental and neurodegenerative diseases using human induced pluripotent stem cells. J Neurogenet. 2014; 28:5–29. [PubMed: 24628482]

Stover AE, Schwartz PH. Adaptation of human pluripotent stem cells to feeder-free conditions in chemically defined medium with enzymatic single-cell passaging. Methods Mol Biol. 2011a; 767:137–146. [PubMed: 21822872]

Stover, AE., Schwartz, PH. The generation of embryoid bodies from feeder-based or feeder-free human pluripotent stem cell cultures. In: Schwartz, PH., Wesselschmidt, RL., editors. Human Pluripotent Stem Cells: Methods and Protocols. Humana Press; Totowa, NJ: 2011b. p. 391-398.

Stover AE, Brick DJ, Nethercott HE, Banuelos MG, Sun L, O'Dowd DK, Schwartz PH. Process-based expansion and neural differentiation of human pluripotent stem cells for transplantation and disease modeling. J Neurosci Res. 2013; 91:1247–1262. [PubMed: 23893392]

Sun Y, Florer J, Mayhew CN, Jia Z, Zhao Z, Xu K, Ran H, Liou B, Zhang W, Setchell KD, Gu J, Grabowski GA. Properties of neurons derived from induced pluripotent stem cells of Gaucher disease type 2 patient fibroblasts: potential role in neuropathology. PLoS One. 2015; 10:e0118771. [PubMed: 25822147]

Sun Y, Pasca SP, Portmann T, Goold C, Worringer KA, Guan W, Chan KC, Gai H, Vogt D, Chen YJ, Mao R, Chan K, Rubenstein JL, Madison DV, Hallmayer J, Froehlich-Santino WM, Bernstein JA, Dolmetsch RE. A deleterious Nav1.1 mutation selectively impairs telencephalic inhibitory neurons derived from Dravet Syndrome patients. elife. 2016:5.

Suzuki IK, Vanderhaeghen P. Is this a brain which I see before me? Modeling human neural development with pluripotent stem cells. Development. 2015; 142:3138–3150. [PubMed: 26395142]

Tang X, Zhou L, Wagner AM, Marchetto MC, Muotri AR, Gage FH, Chen G. Astroglial cells regulate the developmental timeline of human neurons differentiated from induced pluripotent stem cells. Stem Cell Res. 2013; 11:743–757. [PubMed: 23759711]

Xue M, Atallah BV, Scanziani M. Equalizing excitation-inhibition ratios across visual cortical neurons. Nature. 2014; 511:596–600. [PubMed: 25043046]

Yan Y, Shin S, Jha BS, Liu Q, Sheng J, Li F, Zhan M, Davis J, Bharti K, Zeng X, Rao M, Malik N, Vemuri MC. Efficient and rapid derivation of primitive neural stem cells and generation of brain subtype neurons from human pluripotent stem cells. Stem Cells Transl Med. 2013; 2:862–870. [PubMed: 24113065]

Yang N, Ng YH, Pang ZP, Südhof TC, Wernig M. Induced neuronal cells: how to make and define a neuron. Cell Stem Cell. 2011; 9:517–525. [PubMed: 22136927]

Yuan F, Fang KH, Cao SY, Qu ZY, Li Q, Krencik R, Xu M, Bhattacharyya A, Su YW, Zhu DY, Liu Y. Efficient generation of region-specific forebrain neurons from human pluripotent stem cells under highly defined condition. Sci Rep. 2015; 5:18550. [PubMed: 26670131]

Zhang Y, Pak C, Han Y, Ahlenius H, Zhang Z, Chanda S, Marro S, Patzke C, Acuna C, Covy J, Xu W, Yang N, Danko T, Chen L, Wernig M, Sudhof TC. Rapid single-step induction of functional neurons from human pluripotent stem cells. Neuron. 2013; 78:785–798. [PubMed: 23764284]
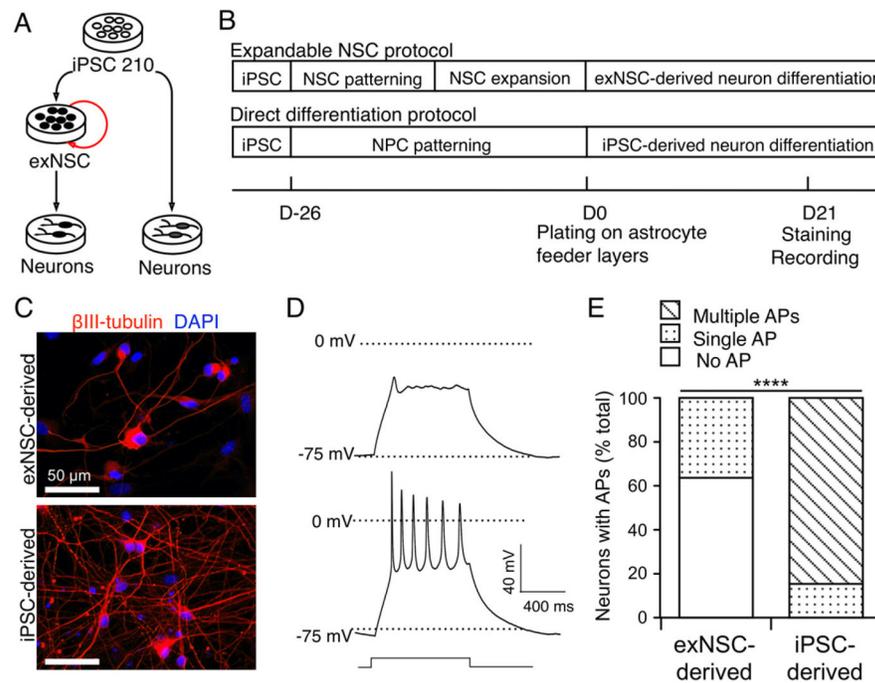
Fig. 1.

Maturation of excitability is faster in hiPSC-derived neurons than in expandable NSC-derived neurons. (A) Flowchart of the two protocols utilized to generate neurons derived from the control hiPSC line 210. (B) The expandable NSC protocol includes generating an intermediate, regenerative population of neural stem cells (exNSCs) from the hiPSCs that are expanded before being differentiated into neurons. In the direct differentiation protocol, hiPSCs are patterned into neural progenitor cells (NPCs) that are directly differentiated, without expansion, into neurons. exNSCs and NPCs are both plated at the same density onto mouse cortical astroglia feeder layers to promote neuronal differentiation. (C) Immunostaining (D21 post plating) with a neuronal marker βIII-tubulin and a nuclei marker DAPI in exNSC- and hiPSC-derived cultures. (D) Representative recordings of typical evoked firing from exNSC- and hiPSC-derived neurons (D21 post plating). (E) The proportion of neurons that fired no action potentials (AP), a single AP or multiple APs was significantly different in exNSC- and hiPSC-derived neurons ($p < 0.0001$, Chi-square test, n = 22 exNSC-derived neurons and n = 26 hiPSC-derived neurons recorded at D21 post plating).
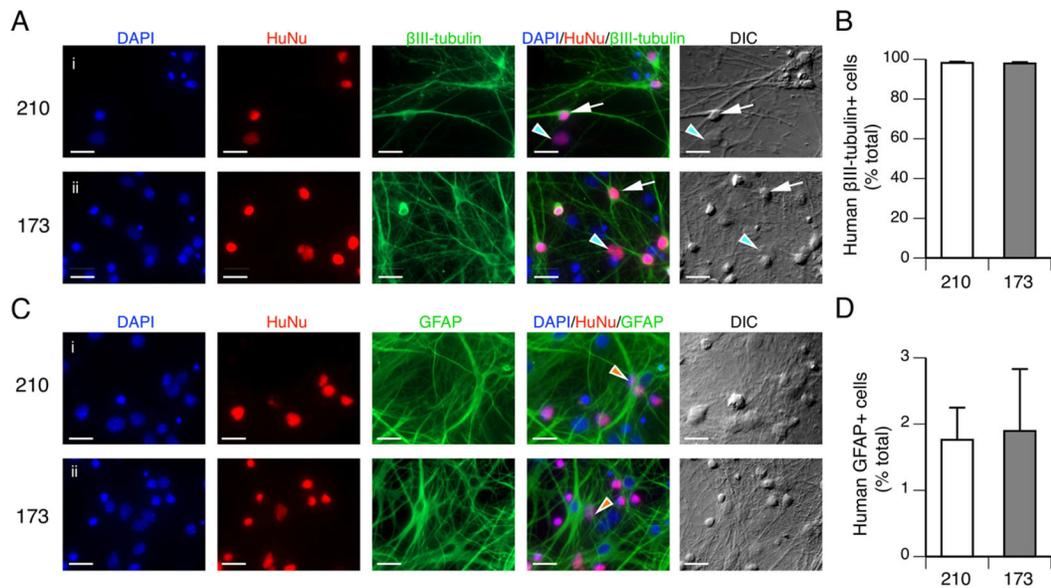
Fig. 2.
Direct differentiation of hiPSCs results in primarily neurons. (A) Immunostaining of control 210 and 173 hiPSC-derived cultures by DAPI, HuNu and βIII-tubulin antibodies at 3 weeks post plating. HuNu positive, βIII-tubulin positive cells are indicated by white arrows. HuNu positive, βIII-tubulin negative cells indicated by light blue arrowheads. (B) The proportion of hiPSC-derived neurons in cultures of control 210 and 173 at 3 weeks post plating. (C) Immunostaining of control 210 and 173 hiPSC-derived cultures by DAPI, HuNu and GFAP antibodies at 3 weeks post plating. HuNu positive, GFAP positive cells are indicated by orange arrowheads. DAPIpositive HuNu negative identifies nuclei of mouse cells in the feeder layers that are enriched for astrocytes stained by GFAP. (D) The proportion of hiPSC-derived astrocytes in cultures of control 210 and 173 at 3 weeks post plating. Data represented as mean + s.e.m. Three coverslips from each of the two individual platings of each line were included. No significant difference in the percentage of hiPSC-derived neurons and astrocytes in the two lines, p > 0.75, unpaired *t*-test with Welch's correction.
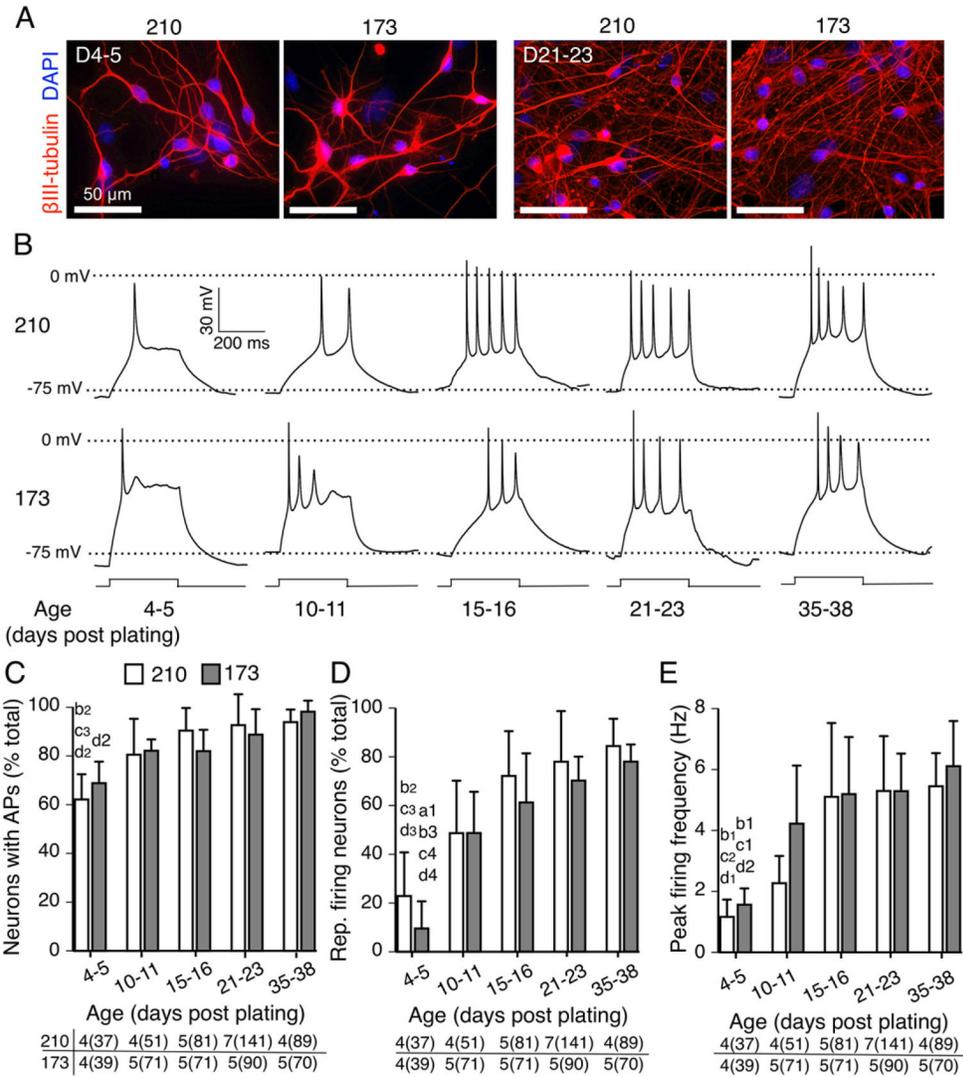
Fig. 3.
Intrinsic firing properties of hiPSC-derived neurons mature at a similar rate from plating to plating in control lines, and between control hiPSC lines 210 and 173. (A) Immunostaining with βIII-tubulin antibody and DAPI on neurons derived from control hiPSC 210 and 173 at D4–5 and D21–23 post plating. (B) Representative traces of action potentials evoked in control hiPSC 210- and 173-derived neurons in response to a 600 ms depolarizing current pulse at five recording windows between 4 and 38 days post plating. (C) The percentage of neurons capable of evoked firing, (D) repetitive firing (>2 APs) and (E) the peak firing frequency as a function of age. Data are reported as mean + SD. Number of individual platings at each time window from 2 lines is reported in the bottom of C–E with number of neurons in parentheses. All three properties were significantly different as a function of age (two-way ANOVA with *post hoc* Bonferroni test, results in Table 3). a, b, c and d denote significance from D10–11, D15–16, D21–23 and D35–38 post plating respectively within the same line. Numbers next to the letters represent degrees of significance with 1, 2, 3 and 4
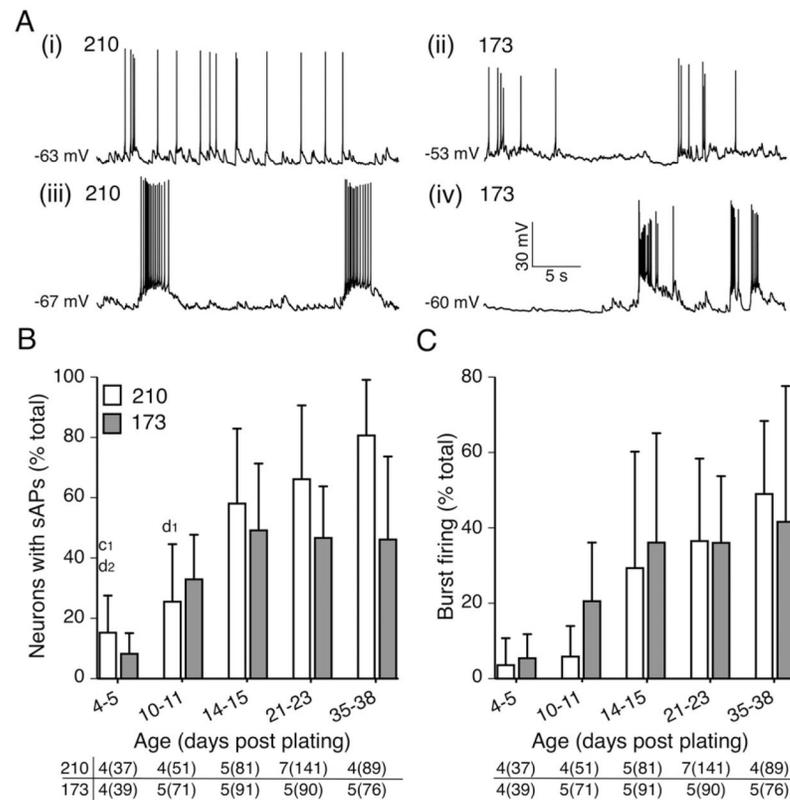
denoting p value < 0.05, 0.01, 0.001 and 0.0001 respectively. There was no significant difference between cell lines (Table 3).

Fig. 4.
hiPSC-derived neurons in both 210 and 173 lines are spontaneously active. (A) Spontaneous firing patterns classified as irregular tonic firing (i and ii) or burst firing (iii and iv) in hiPSC 210- and 173-derived neurons. RMP is indicated at the baseline of each trace. (B) The percentage of neurons exhibiting spontaneous firing (C) or the subset with burst firing (D) at 5 time windows over 5 weeks. Data are represented as mean + SD. Number of individual platings at each time window from 2 lines is reported in the bottom of B and C with number of neurons in parentheses. Two-way ANOVA (results in Table 3) with *post hoc* Bonferroni test. c and d denote significance from D21–23 and D35–38 post plating respectively within the same line. Numbers next to the letters represent degree of significance with 1 and 2 denoting p value < 0.05 and 0.01 respectively.
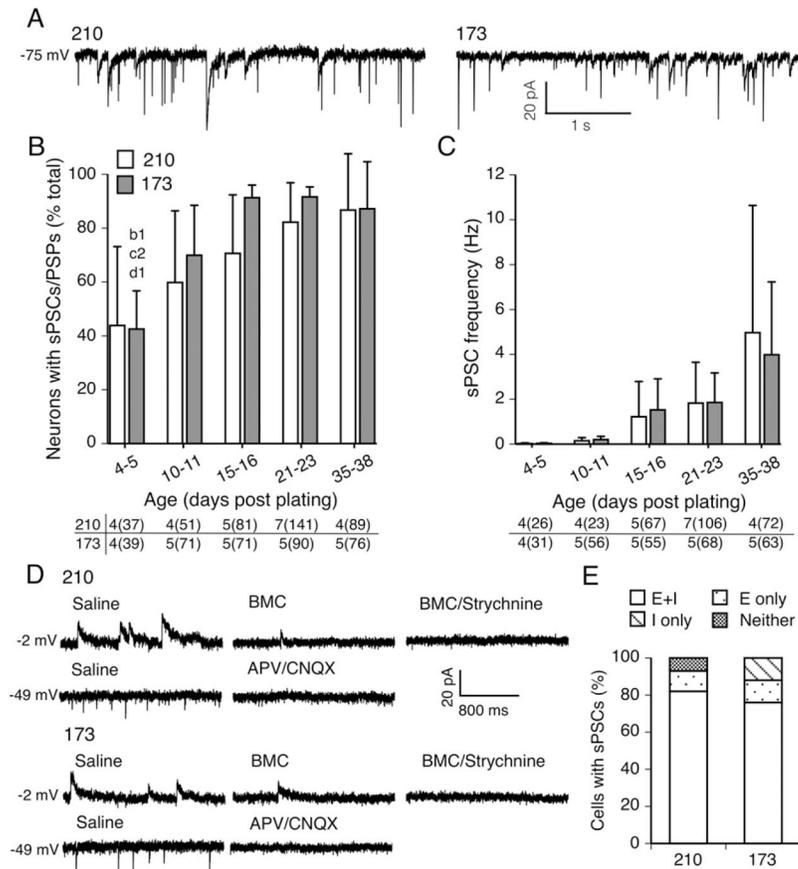
Fig. 5.
Functionally active networks of synaptically connected excitatory and inhibitory cells in cultures from both control hiPSC lines. (A) Representative traces of sPSCs in neurons derived from control hiPSC lines 210 and 173. Holding potential −75 mV. (B) The percentage of neurons exhibiting sPSCs as a function of age in culture. (C) Developmental increase in sPSC frequency in neurons from control hiPSC 210 and 173. Data are reported as mean + SD. Number of individual platings at each time window from 2 lines is reported in the bottom of B and C with number of neurons in parentheses. Two-way ANOVA with *post hoc* Bonferroni test (results in Table 3). b, c, and d denote significance from D15–16, D21–23 and D35–38 post plating, respectively, within the same line. Numbers next to the letters represent degrees of significance with 1 and 2 denoting p value < 0.05 and 0.01 respectively. (D) Characterization of sEPSCs at the presence of glutamate receptor blockers APV and CNQX at −49 mV and sIPSCs at the presence of $GABA_A$ receptor blocker BMC and glycine receptor blocker strychnine at −2 mV in neurons from 210 (top) and 173 (bottom) lines at D21–23 post plating. (E) Proportion of neurons from 210 and 173 hiPSC lines with both sEPSCs and sIPSCs at D21–23 post plating. n = 25 and n = 27 neurons from lines 210 and 173 respectively.
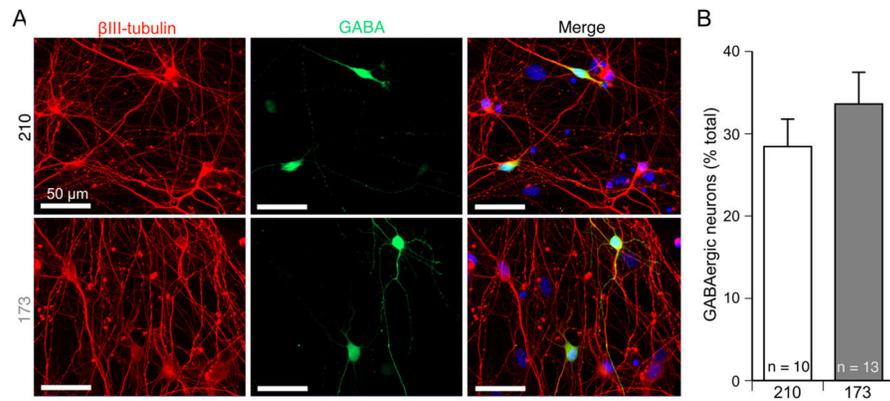
Fig. 6.
Cultures from 210 and 173 contain a similar percentage of GABAergic neurons. (A)
Cultures differentiated from the control 210 and 173 hiPSC-derived neurons were stained
with nuclei marker DAPI, βIII-tubulin and GABA antibodies to identify GABAergic
neurons at D21 post plating. (B) The proportion of GABAergic neurons in neuronal cultures
of control 210 and 173 at D21 post plating. Data represented as mean + s.e.m. Number of
coverslips from each line indicated on the graph. There was no significant difference in the
percentage of GABAergic neurons in the two lines, $p > 0.14$, unpaired t-test with Welch's
correction.

Table 1

Passive membrane properties of neurons generated by an expandable NSC protocol and a direct differentiation protocol.

	exNSC-derived neurons	hiPSC-derived neurons
R_m (GΩ)	1.9 ± 2	1.8 ± 1.0
RMP (mV)	−59 ± 12	−57 ± 10
C_m (pF)	12 ± 4	32 ± 7 [***]

Data reported as mean ± SD.

[***] represents p < 0.0001, unpaired *t*-test with Welch's correction.

n = 22 for exNSC-derived neurons and n = 26 for hiPSC-derived neurons.

Table 2

Passive membrane properties of directly differentiated neurons from control hiPSC lines 210 and 173.

	Line	Days post plating				
		4–5	10–11	15–16	21–24	35–38
R_m (GΩ)	210	2.6 ± 0.4	2.5 ± 0.2	2.2 ± 0.4	1.6 ± 0.5	1.4 ± 0.4
		4(36)	5(51)	5(81)	7(131)	4(101)
	173	2.7 ± 0.6	2.3 ± 0.4	1.9 ± 0.3	1.7 ± 0.2	1.2 ± 0.2
		4(39)	6(47)	6(48)	6(65)	6(52)
RMP (mV)	210	-53.5 ± 8.4	-50.8 ± 6.4	-55.1 ± 4.5	-54.1 ± 3.6	-53.4 ± 4.1
		4(36)	5(51)	5(81)	7(131)	4(101)
	173	-50.2 ± 2.3	-50.0 ± 3.2	-54.7 ± 5.0	-50.1 ± 2.5	-48.6 ± 2.7
		4(39)	6(47)	6(48)	6(65)	6(52)
C_m (pF)	210	25.5 ± 3.0	25.2 ± 3.2	33.0 ± 5.2[a]	37.0 ± 8.5[b]	43.5 ± 15.9
		4(36)	5(51)	5(81)	7(131)	4(101)
	173	15.1 ± 1.8	19.0 ± 2.2	19.1 ± 3.2[a]	23.4 ± 1.8[b]	34.4 ± 3.7
		4(31)	6(58)	6(50)	6(63)	6(69)

Data reported as mean ± SD with number of individual platings (total number of neurons).

[a] $p < 0.01$.

[b] $p < 0.001$, denotes significance between cell lines at given time point post plating (two-way ANOVA with Bonferroni *post hoc* test).

Table 3

Summary of two-way ANOVA statistical analyses on directly differentiated neurons from control hiPSC line 210 and 173.

	Age	Line	Interaction
Evoked firing (% total)	**** (p < 0.0001)	ns (p = 0.98)	ns (p = 0.40)
Multiple firing (% total)	**** (p < 0.0001)	ns (p = 0.10)	ns (p = 0.92)
Firing frequency	**** (p < 0.0001)	ns (p = 0.17)	ns (p = 0.59)
sAP (% total)	**** (p < 0.0001)	* (p = 0.03)	ns (p = 0.22)
Burst sAP (% total)	** (p = 0.0014)	ns (p = 0.63)	ns (p = 0.84)
sPSC/PSPs (% total)	**** (p < 0.0001)	ns (p = 0.13)	ns (p = 0.67)
sPSC frequency	*** (p = 0.0004)	ns (p = 0.85)	ns (p = 0.97)
R_m	**** (p < 0.0001)	ns (p = 0.33)	ns (p = 0.55)
RMP	ns (p = 0.18)	* (p = 0.04)	ns (p = 0.72)
C_m	**** (p < 0.0001)	**** (p < 0.0001)	ns (p = 0.53)

Two-way ANOVA utilized to examine effects of age (days post plating), cell line identity, and interaction between both.

*, **, ***, and **** reflect p < 0.05, 0.01, 0.001 and 0.0001 respectively.